JOURNAL OF MATERIALS SCIENCE **32** (1997) 5347–5354

Fracture resistance of polyblends and polyblend matrix composites

Part II *Role of the rubber phase in nylon 6,6/ABS alloys*

S. V. NAIR, A. SUBRAMANIAM
Department of Mechanical Engineering, University of Massachusetts, Amherst, MA 01003, USA

L. A. GOETTLER
Vydyne Tech Center, The Chemical Group, Monsanto Company, Cantonment, FL 32533, USA

A comprehensive study was undertaken on the specific role of rubber on toughening when other rigid polymer or non-polymer phases were present. Nylon 6,6/SAN blends of various SAN concentrations ranging from pure SAN to pure nylon 6,6 were investigated with and without fibre reinforcements. These results could be compared with the toughness values of unreinforced and fibre-reinforced nylon 6,6/ABS alloys from a previous study in order to elucidate the role of rubber. Fracture behaviour was investigated rigorously by characterizing the fracture initiation toughness, J_{IC}, and the steady-state fracture toughness, J_{SS}. These were then related to the microstructure and failure modes determined by microscopy and fractography methods. It was found that rubber increased both fracture initiation and propagation toughness in the presence of the rigid phase, while the rigid phase toughened the alloy only when the rigid phase/matrix interface was strong enough. The role played by glass fibres was found to be critically related to the fibre/matrix interfacial strength. Toughening was generally observed, both in the presence and absence of rubber, when the interface was strong. In all cases toughening could be related to the enhancement of plasticity in the crack tip by the presence of the rubber phase or the reinforcing glass phase.

1. Introduction

Engineering thermoplastics have relatively poor fracture toughness levels when compared to other classes of materials like metals and ceramics. One method of toughening them has been by blending them with an elastomeric phase [1–11]. Here, the toughening mechanism is believed to be the relief of crack-tip stress triaxiality by cavitation of the elastomeric phase, which in turn promotes shear yielding in the surrounding matrix phase [3, 12]. A variety of factors such as rubber concentration, particle size, interparticle distance and temperature are known to affect the toughening process and these have been studied extensively [13–15].

Part I [16] examined the role of a second rigid phase on rubber toughening by studying nylon 6,6/ABS blends having various concentrations of ABS both with and without fibre reinforcements. The rigid phases were therefore, polyamide 6,6 (nylon 6,6), styrene acrylonitrile (SAN) and glass fibres. It was shown that in the presence of a second rigid polymer phase, embrittlement effects were evident. In other words, nylon 6,6 as a minor second phase was observed to reduce the fracture toughness of ABS and ABS as a minor second phase reduced the fracture toughness of nylon 6,6. In contrast, addition of fibres to the rubber-containing blends of nylon 6,6 and ABS was found to increase fracture toughness. Because none of the blends or their composites were studied in the absence of rubber, the specific role of rubber could not be clarified in that study [16].

In this paper, a comprehensive study is reported of the specific role of rubber on toughening when other rigid polymer or non-polymer phases were present. Nylon 6,6/SAN blends of various SAN concentrations ranging from pure SAN to pure nylon 6,6 were investigated with and without fibre reinforcements. These results could be compared to the toughness values of unreinforced and fibre-reinforced nylon 6,6/ABS alloys from the previous study [16], in order to elucidate the role of rubber. As in that study [16], fracture behaviour was investigated rigorously by characterizing the fracture initiation toughness, J_{IC}, and the steady-state fracture toughness, J_{ss}. These were then related to the microstructure and failure modes determined by microscopy and fractography methods. It should be mentioned that the results relating to the nylon 6,6/ABS systems, which are used in this paper, were obtained from the previous study [16].

2. Experimental procedure

2.1. Materials

The materials used in this study were processed at Monsanto Chemical Company, Springfield, MA. The raw materials used were poly(hexamethylene adipamide) or nylon, 6,6, styrene acrylonitrile (SAN), glass fibres and a maleic anhydride type of nylon 6,6/SAN compatibilizer. The glass fibres used were Star Stran 702, for the nylon 6,6-rich materials. and Star Stran 726, for the SAN-rich materials. Star Stran 702 and 726 are E-type glass fibres, compatible with nylon 6,6 and SAN, respectively, manufactured by Schuller Mats and Reinforcements. The glass fibres were added to the extent of 16 vol % of the total filled polymer. The materials which were processed were pure SAN, 20/80 nylon 6,6/SAN and 80/20 nylon 6,6/SAN, where the ratios are given in terms of the relative weight percentages. Glass fibre-reinforced composites were also processed with the above materials as matrices. The appropriate amounts of the different components were compounded together in a 34 mm co-rotating/intermeshing American Leistritz twin-screw extruder. Zone sets varying from 220–260 °C were used, with a vacuum of 28 in ($\sim$ 711 mm) Hg. The extruded blends were then dried at 80 °C for 18 h in a Conair desiccant bed system. Injection moulding of these blends was carried out using an Engel EC88 machine, with a mould temperature of around 50 °C and an injection pressure of 900–1250 p.s.i. (10^3 p.s.i. $=$ 6.89 N mm^{-2}). Higher moulding temperatures and pressures were used for the fibre-reinforced blends in order to improve flow. Tensile specimens $\frac{1}{8}$ in ($\sim$ 3 mm) thick and bend bars $\frac{1}{4}$ in ($\sim$ 6 mm) thick were made. In order to prevent the effects of moisture, the specimens were sealed first in plastic bags and then in aluminized paper.

2.2. Mechanical properties and microstructural evaluation

Tensile tests were carried out according to ASTM D638 on a computer-controlled Instron model 1321 servohydraulic testing machine. The J-integral initiation toughness, J_{IC}, was determined using a new protocol proposed by the ASTM task force [17]. Three-point bend specimens were used with a span-to-width ratio of 4 ($L = 5.08$ cm, $W = 1.27$ cm, thickness, $B = 0.64$ cm). A saw cut was used to create the single-edge initial notch for these specimens. Pre-cracks were created by sliding a sharp microtome blade into the notch. After a 2 d period of stress relaxation, these specimens were loaded on the Instron to different values of load point displacements. The specimens were then unloaded, immersed in liquid nitrogen, and fractured by loading on the Instron at a very high rate. The amount of crack extension was measured using a stereo-microscope and the J-integral fracture resistance, J_{R}, was calculated using the relation

$$J_{\mathrm{R}} = \frac{2U}{Bb} \qquad (1)$$

where U is the area under the load–displacement curve, B is the thickness and b is the ligament length. J_{IC} was determined from the J_{R}–Δa curve using the 0.2 mm offset prescribed by the protocol. The specimen thickness values needed for valid plane strain toughness measurements were also checked according to the ASTM recommended values of

$$B \geqslant \frac{25 J_{\mathrm{Q}}}{\sigma_{\mathrm{y}}} \qquad (2)$$

where B is the thickness, W is the width of the specimen, J_{Q} is the measured value of toughness and σ_{y} is the material yield stress.

The J-integral steady state toughness, J_{ss}, refers to the plateau value of the material R-curve and its significance was discussed in detail in Part I [16]. J_{ss} was measured by using a modification of the technique proposed by Li and co-workers [18–20]. Two identical three-point bend specimens with incrementally different initial crack lengths were loaded until the two curves came together. For two identical specimens, which differ only in their initial crack sizes by Δa, the J_{R} curve is defined according to the relation

$$J_{\mathrm{R}} = \frac{A(\delta)}{B(\Delta a)} \qquad (3)$$

where $A(\delta)$ is the area between the two load–displacement curves at a load point displacement of δ, and B is the thickness of the specimens. The steady-state value, J_{ss}, corresponds to the point when the two P–δ curves come together. Plane strain thickness requirements for the J_{ss} values were also checked on the basis of Equation 2, where J_{Q} was set equal to J_{ss}. Kim and Joe [21] have used a similar method to determine the plateau value of crack growth resistance, which they named "R_{P}". They also established it to be a geometry-independent parameter.

The fracture surfaces of the specimens were examined using a Jeol-JSMS5410 scanning electron microscope, after loading SENB specimens at 1 mm min^{-1}. The specimens were coated with a thin layer of gold in order to improve conductivity of the surface and prevent electron charging.

3. Results and discussion

3.1. Initiation toughness

3.1.1. Role of rubber

Comparing the fracture initiation toughness of nylon, 6,6/ABS blends with that of the nylon, 6,6/SAN case (Fig. 1), it is evident that addition of rubber phase to the nylon 6,6/SAN system increased fracture toughness. This increase was roughly the same at all blend compositions, approximately 3–4 kJ m^{-2}, indicating that rubber provided essentially an additive toughness increase irrespective of blend composition. Note that the data for the 50/50 nylon 6,6/ABS blend composition from Part I [16] were omitted from the figure because this composition was not studied in the present work. Accordingly, these conclusions hold when the second minor component is discontinuous. As was pointed out [16], the 50/50 nylon 6,6/ABS blend was co-continuous in character and consequently, cannot be compared with the present results.

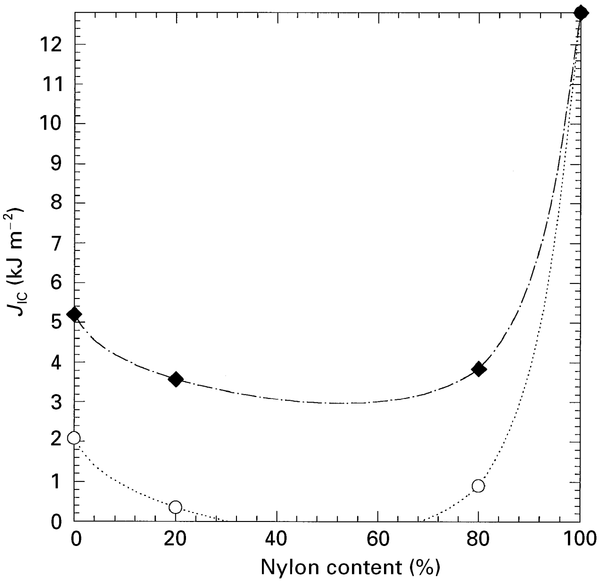

Figure 1 Fracture initiation toughness versus blend composition for the unreinforced alloys: (○) no rubber, (◆) ABS [16].

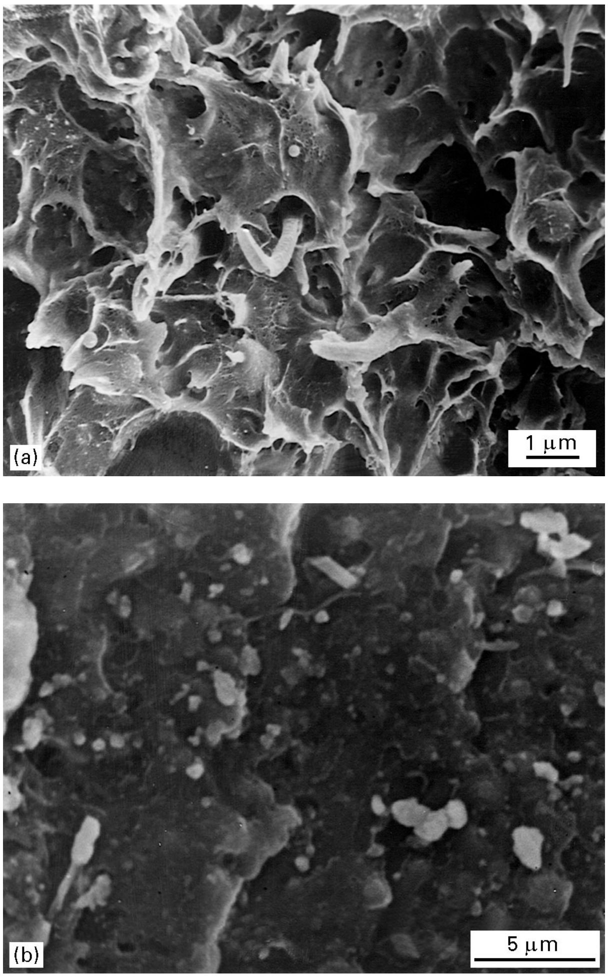

Figure 2 SEM fractograph of (a) 20/80 nylon 6,6/ABS, from [16], and (b) of 20/80 nylon 6,6/SAN, from this study.

The increase in toughness resulting from the presence of rubber is evident, for example, from the enhanced plasticity in the crack-tip region of the 20/80 nylon 6,6/ABS, Fig. 2a, compared to that in the 20/80 nylon 6,6/SAN case, see Fig. 2b. In the latter, SAN fractures in a relatively brittle fashion, whereas in the ABS case, it is clear that the rubber induced significant plasticity in the surrounding SAN. As has been discussed extensively before [16], this enhanced plasticity apparently derives from the ability of the rubber particles containing occluded SAN to cavitate and thereby promote shear yielding in the surrounding SAN. The same result of rubber-induced plasticity was also observed in the 80/20 nylon 6,6/ABS system on comparing with the 80/20 nylon 6,6/SAN system, see Fig. 3a and b.

It should be pointed out here that in the 20/80 system, the size and distribution of the second-phase nylon 6,6 were equivalent in the two systems. The only difference was that in the 20/80 nylon 6,6/ABS the nylon 6,6 phase had an elongated morphology. In the 80/20 system the second phase, SAN, roughly had the same size and distribution in the nylon 6,6/SAN alloys as in the nylon 6,6/ABS alloys. Accordingly, the differences in toughness were not attributed to microstructural differences but rather to the presence or absence of the rubber phase.

3.1.2. Role of second rigid phase

A second clear conclusion when comparing the toughness of nylon 6,6/ABS to that of the nylon 6,6/SAN case (Fig. 1) was that the second rigid phase apparently embrittled the blend, that is, caused a decrease in J_{IC}. This embrittling effect was observed both when nylon 6,6 was added as a minor phase to SAN and also when SAN was added as a minor phase to nylon 6,6. This embrittling effect was observed to approximately the same degree in the nylon 6,6/ABS system as well, that is, addition of ABS to nylon 6,6 decreased the toughness of the nylon 6,6 phase and likewise, addition of nylon 6,6 to ABS decreased the toughness of the ABS phase, roughly to the same extent as they did when rubber was absent. This indicated that the toughness decrease was indeed the result of an interaction between the rigid phases and was not directly related to the rubber phase.

The embrittling effect of the second rigid phase, was attributed to debonding at the interfaces between the rigid phases as a result of concentration of stress at these interfaces. This can be clearly observed on the fracture surfaces. In the case when SAN was added to nylon 6,6, the interfaces were severely debonded, see Fig. 3b, whereas when nylon 6,6 was added to SAN, debonding occurred, but was far less severe, see Fig. 2b. It is to be expected, that from a mechanics standpoint, a higher modulus phase in a lower modulus matrix would produce higher stress concentrations because the high-modulus minor phase would then impede deformation in the surrounding lower modulus matrix phase. From the tensile tests the modulus values of nylon 6,6, SAN and ABS were found to be around 1260, 1600 and 1380 MPa, respectively. This is consistent with the observed results, namely, that SAN, which has a much higher modulus than nylon 6,6, was the stronger embrittling agent.

The above argument raises the expectation that increasing the strength of the rigid/rigid polymer

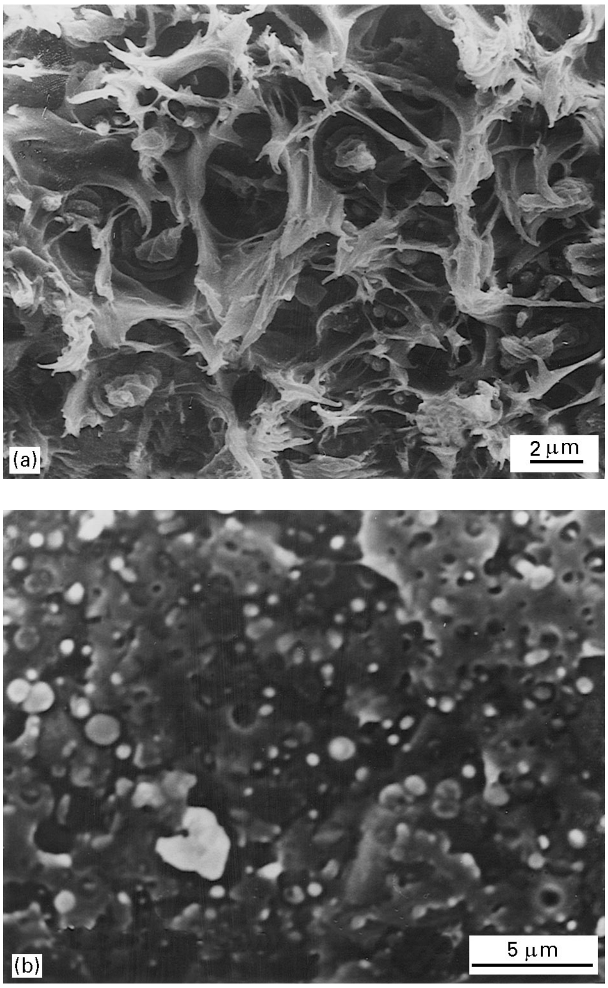

Figure 3 SEM fractograph of (a) 80/20 nylon 6,6/ABS, from [16], and (b) 80/20 nylon 6,6/SAN, from this study.

interfaces could preclude toughness reduction. Indeed, consistent with this expectation, it was found [16] that the fracture toughness of the 20/80 nylon 6,6/ABS increased as the content of the compatibilizer between SAN and nylon 6,6 phase was increased. In fact, at high enough compatibilizer content, the fracture toughness of the nylon 6,6/ABS was greater than that of the ABS itself. Clearly, this further suggests that, provided that the rigid/rigid interface is sufficiently strong, rigid-phase toughening can also result. This result appears to be related, in part, to the role of the rigid phase in determining the plasticity in the surrounding matrix. When the interface is relatively weak, debonding at the interface can cause damage-induced embrittlement; however, when the interface is strong, there is potential for the second rigid phase to actually promote localized plasticity which in turn improves toughness. This mechanism was discussed recently by Shiao *et al.* [22] and in Part I [16] of this series. It is also borne out by the fibre-toughening results of this study, see below.

3.1.3. Role of glass fibres

The corresponding fracture initiation toughness results for fibre-reinforced nylon 6,6/ABS and fibre-reinforced nylon 6,6/SAN are compared in Fig. 4. It is evident by comparing Fig. 4 with the previous case, namely Fig. 1, that the fibres by themselves as a particular form of rigid phase tended to increase significantly the toughness corresponding to the case when fibres were not present. This was found to take place only when the matrix was a blend of two rigid phases. In the case of pure nylon 6,6, for example, a substantial decrease in toughness resulted from fibre additions, whereas toughness was essentially the same for pure ABS and pure SAN on fibre additions. Fractographic observations showed rather clean fibre surfaces on pulled out fibres for the pure materials, that is, nylon 6,6, SAN and ABS. An example is shown in Fig. 5; as very clean or smooth pulled-out fibre surfaces for the case of fibre-reinforced SAN are seen. This suggests a weak fibre/matrix interface. However, for the case when the matrix was a blend of two rigid phases, the fibre surfaces appeared to contain adhering matrix phase, suggesting a stronger fibre/matrix

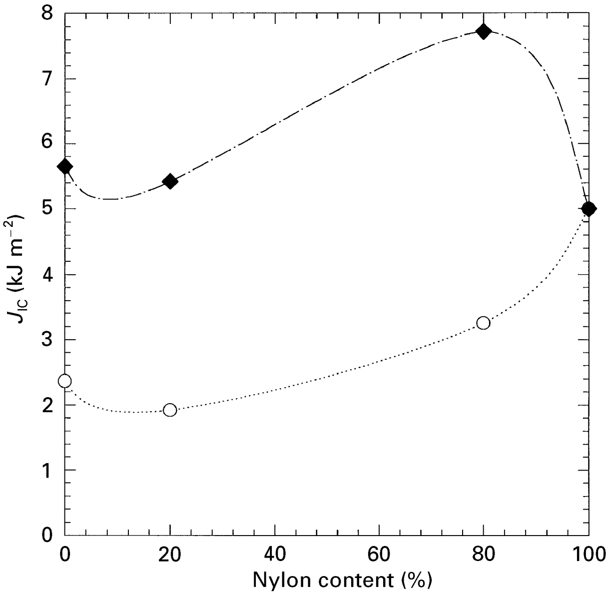

Figure 4 Fracture initiation toughness versus alloy composition for fibre-reinforced alloys: (○) no rubber, (◆) ABS [16].

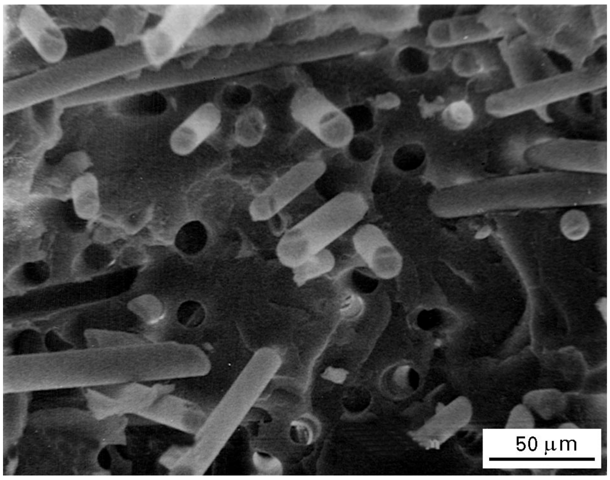

Figure 5 SEM fractograph of fibre-reinforced SAN showing relatively clean surfaces of pulled-out fibres.

interface, see for example, Fig. 6a and b which show evidence of strong fibre/matrix interfaces in fibre-reinforced 20/80 nylon 6,6/SAN and fibre-reinforced 80/20 nylon 6,6/SAN. Once again, it appeared that when the rigid phase, in this case, the fibre phase, was sufficiently well bonded to the matrix, toughening can result, even when the matrix is rigid (non-elastomeric).

The reason for achieving a higher fibre–matrix interface strength in the blends containing a second rigid phase minor component, is not clear. The fibres in this study were compatibilized with the major phase and so one would expect a similar strength between the fibre and matrix in the fibre-reinforced SAN as well as in the fibre-reinforced 20/80 nylon 6,6/SAN alloys. Yet, the latter appeared to display higher strengths. As mentioned in the previous paper [16], the same result was observed in the nylon 6,6/ABS system as well. This result was observed to be true in all cases except one (to be discussed later). More study is needed to clarify the role of blend composition on the fibre/matrix interface characteristics.

The role of the fibres, like that of the rigid polymer phase discussed earlier, also appears to be related in part to the role of the fibres in enhancing the plasticity in the surrounding matrix. Direct experimental evidence of the new role played by fibres in influencing the deforming characteristics of the matrix is shown in Fig. 7 for the case when SAN is the minor phase in the matrix and in Fig. 8 when nylon 6,6 is the minor phase in the matrix. Comparing the fracture surface of the unreinforced material (Figs 2b and 3b) with the matrix region of the corresponding fibre-reinforced material (Figs 7 and 8), it appeared that the composite matrix experienced enhanced plastic deformation. This enhancement of matrix plasticity can in and of itself enhance the fracture initiation toughness. Such an effect was also observed and discussed in a composite with an ABS type of matrix by Nair *et al.* [23] and was also noted in the previous paper [16]. Thus, enhancement of matrix plasticity by fibres does not apparently require the presence of an elastomeric phase. Rigid matrices can also exhibit enhanced shear yielding.

The reason for the enhancement of plasticity was attributed to the fact that the presence of fibres increases the shear stress in the surrounding matrix. Thus, fibres can play the role much like that of rubber in reducing the hydrostatic stress state and increasing the deviatoric stress resulting in fibre toughening. Indeed Shiao *et al.* [24] recently found analogies between fibre toughening and rubber toughening in fibre-reinforced nylon 6,6 composites, in support of this model. It appeared that such toughening

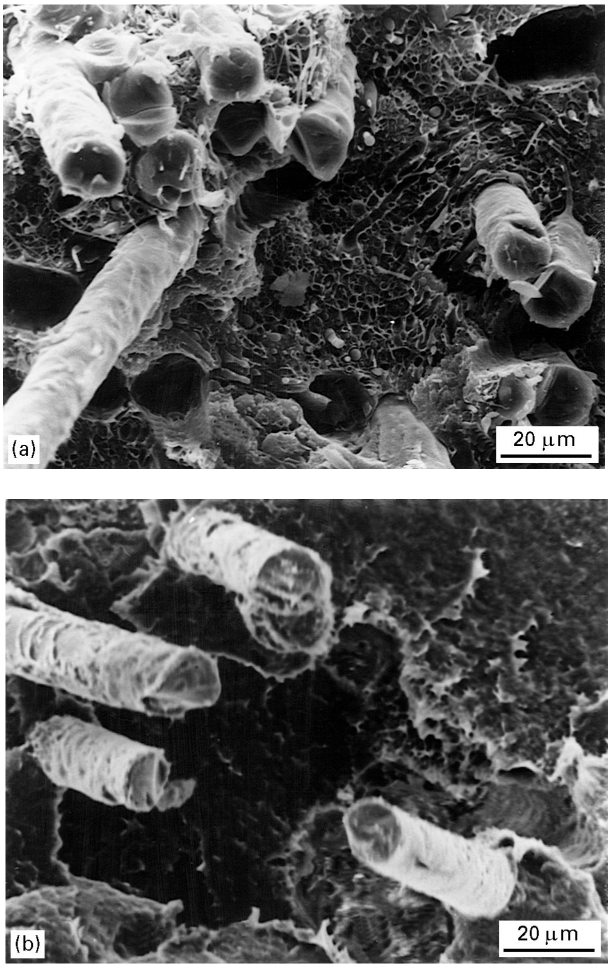

Figure 6 SEM fractograph of fibre-reinforced (a) 20/80 and (b) 80/20 nylon 6,6/SAN matrices showing evidence of a strong fibre/matrix interface.

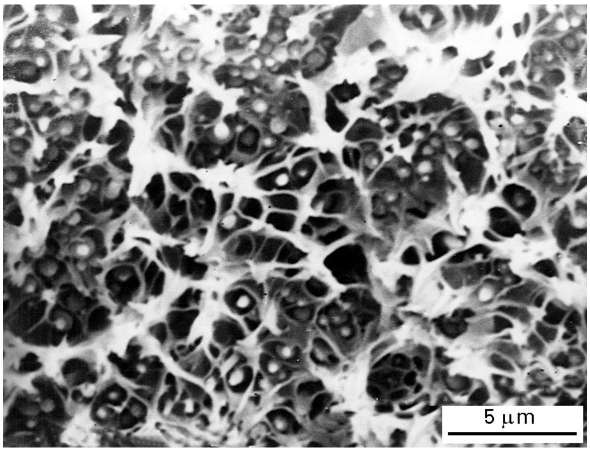

Figure 7 SEM fractograph of the fracture surface of the matrix region of fibre-reinforced 80/20 nylon 6,6/SAN.

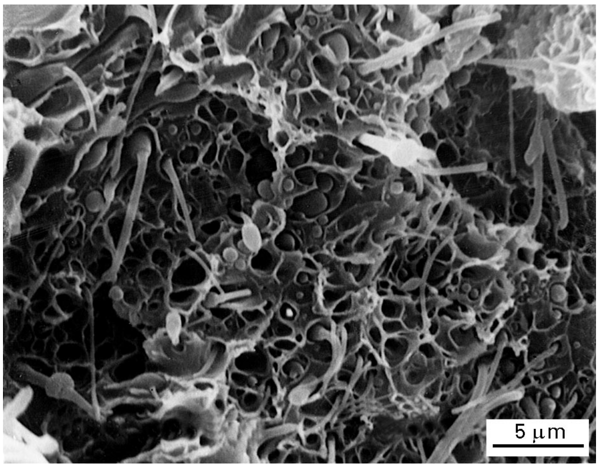

Figure 8 SEM fractograph of the fracture surface of the matrix region of fibre-reinforced 20/80 nylon 6,6/SAN.

processes are operative in the nylon 6,6 blends as well, not just in the pure nylon 6,6 case.

The second question regarding the case when fibres are present concerns the role of the rubber phase and the role of the second rigid phase. With regard to the role of the rubber phase, it appeared that the rubber phase toughened the composites roughly by an amount on the order of 3–4 kJ m^{-2}, regardless of the blend compositions studied. This can be seen by comparing toughening values of fibre-reinforced nylon 6,6/ABS with the corresponding values for fibre-reinforced nylon 6,6/SAN system, see Fig. 4. This increase was about the same as was observed in the unreinforced case, suggesting that the extent of rubber-phase toughening in ABS was quantitatively the same in the presence and absence of the fibres. This conclusion was further supported by the fact that for a given blend composition, the fibre/matrix interface was observed to be similar in strength, at least qualitatively.

The role of the second rigid phase in the composite is harder to assess because the blend composition changes and consequently, it is expected that the fibre/matrix interface quality could be affected. Therefore, it was not possible unequivocally to separate the role of the second polymer phase from changes in the fibre/matrix interface strength that can cause possible toughening or embrittling effects of the fibres. This effect is illustrated by noting that when SAN was added to the fibre-reinforced nylon 6,6 the toughness decreased, whereas when ABS was added to fibre-reinforced nylon 6,6, the toughness, in contrast, increased. This difference, was not related to any intrinsic role of rubber phase in the ABS, but rather was a result of the fact that fibres substantially decreased the fracture toughness of nylon 6,6 to below that of the fibre-reinforced 80/20 nylon 6,6/ABS blend but above that of the 80/20 nylon 6,6/SAN blend. As was mentioned [16], the decrease in toughness is attributed to a very weak fibre/matrix interface in the fibre-reinforced nylon 6,6 composite.

3.2. Propagation toughness

3.2.1. Role of rubber

Continued stable crack propagation beyond initiation can result from an increase in the crack propagation toughness with crack extension. As was already discussed, J_{ss}, the maximum value of J_R, was used as a measure of the total overall toughness which includes both crack initiation as well as crack propagation components of toughness. The results are shown in Fig. 9. In the first place, no stable crack growth was found in any of the nylon 6,6/SAN blends, so that J_{ss} and J_{IC} were identical for this system, whereas R-curve behaviour was present at all compositions in the presence of ABS. Thus, it was clear that in the unreinforced alloys, it was the presence of rubber that triggered R-curve behaviour and not the presence of the rigid polymer. As we will show in Part III [25], the presence of the rigid polymer was not essential to promote R-curve behaviour when rubber was present. Secondly, it was clear that the crack propagation toughness, or the difference between J_{IC} and J_{ss}, was substantially larger than J_{IC} when rubber was present. Accordingly, all of the fracture propagation toughening in the nylon 6,6/ABS system can be attributed solely to the rubber phase and not to the SAN phase. Also, we can conclude that a predominant role of the rubber, over and above its influence on fracture initiation toughness, was apparently its role in promoting stable crack growth and enhancing the fracture resistance curve or crack propagating toughness. As can be seen from Figs 1 and 9, on addition of rubber, the J_{IC} increased by around 3–4 kJ m^{-2}, whereas the J_{ss} increased by around 12–13 kJ m^{-2}. This indicates the important role played by rubber in crack propagation toughening. This conclusion could not have been arrived at in the previous study [16] because of the absence of the nylon 6,6/SAN data. This important aspect concerning the dominant role of rubber on crack wake effects has not been well recognized to date. Toughening studies by other investigators have tended to concentrate on the crack initiation stage rather than the crack propagation stage and by doing so, the toughening potential of rubber could be substantially underestimated. It should be mentioned here that, as was discussed in the previous paper, the data points for pure ABS and 20/80 nylon 6,6/ABS did not satisfy plane strain requirements and consequently these were plane stress toughness values while the rest were plane strain toughness values. Accordingly, the exact magnitude of the actual plane strain propagation toughness increase in the ABS-rich end is not known.

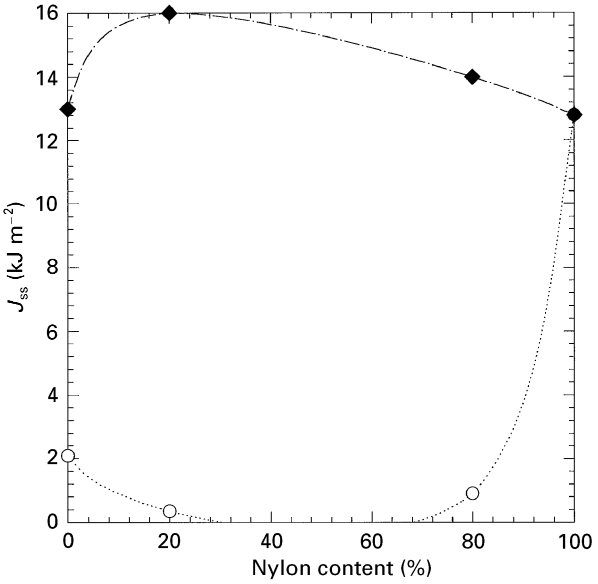

Figure 9 Fracture resistance plateau, J_{ss}, versus alloy composition for the unreinforced alloys: (○) no rubber, (◆) ABS [16].

There have been two proposed mechanistic models for the reason why rubber promotes additional toughening in the crack growth stage. One has to do with the rubber particle bridging in the crack wake [26]. No direct evidence of rubber particle bridging on fracture surfaces was observed in this study. The second model, developed by Evans *et al.* [27], has to do with the fact that rubber-induced plasticity and/or damage is not fully recovered in the wake of the crack, so that the additional non-linear deformation associated with the rubber exerts a closure force on the crack surface in the crack wake. The data obtained in this study were found to be consistent with Evan's model, see Part IV [28].

Note from Fig. 9 that, for the case of pure nylon, no *R*-curve behaviour was induced, either in the presence or the absence of fibres, despite the fact that nylon 6,6 had a relatively high fracture initiation toughness. This issue of when *R*-curve behaviour can be induced was raised in a previous paper [16]. As was discussed there, the absence of *R*-curve behaviour in neat nylon 6,6 may be related to a specimen geometry effect.

3.2.2. Role of glass fibres

Finally, crack propagation toughening in the fibre-reinforced composites is addressed. The propagation toughness results for the composites is shown in Fig. 10. In the absence of rubber, that is, in the nylon 6,6/SAN system fibres always triggered *R*-curve behaviour when the fibre/matrix interface was adequately strong. That is, *R*-curve behaviour was induced by fibres at all compositions except the pure nylon 6,6 case when the interface appeared to be extremely weak [16]. As can be seen, in the composites the total toughness was increased by the presence of rubber for all the blends. For the fibre-reinforced 20/80 nylon 6,6/ABS and fibre-reinforced 20/80 nylon 6,6/SAN, *R*-curve behaviour was observed and addition of rubber resulted in a very substantial increase in propagation toughening. As will be shown in Part IV [28], this is consistent with the role of the rubber in enhancing crack-tip plasticity, as in the case when fibres were absent. Rubber-induced enhancement of local plasticity in the presence of fibres was observed also by Shiao *et al.* [24]. Evidence was presented in that study of shear yield zones generated at rubber particles in the vicinity of glass fibres. As discussed there and in the previous paper [16], this can be attributed to the substantial increase in the deviatoric stress state around glass fibres.

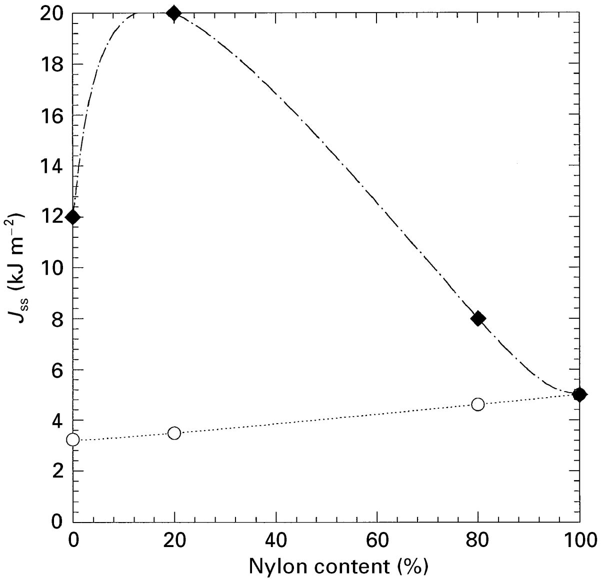

Figure 10 Fracture resistance plateau, J_{ss}, versus matrix alloy composition for fibre-reinforced alloys: (○) no rubber, (◆) ABS [16].

For fibre-reinforced 80/20 nylon 6,6/ABS and fibre-reinforced 80/20 nylon 6,6/SAN, a new and contrasting result was obtained. While *R*-curve behaviour was observed in the 80/20 nylon 6,6/SAN composite, no *R*-curve behaviour was observed in the 80/20 nylon 6,6/ABS composite. This was consistent with the fact that fibre-reinforced 80/20 nylon 6,6/ABS had the highest fracture initiation toughness among the composites and, consequently, could have been more susceptible to a specimen geometry effect. As was pointed out in the previous paper [16], when the fracture initiation toughness is high the increase in the crack driving force may exceed the increase in the fracture resistance as the crack extends. Alternative specimen geometries may need to be used for high-toughness materials in order to characterize their *R*-curve behaviour.

4. Conclusions

1. In all cases, the materials containing rubber were found to be tougher than the materials which did not contain rubber. This was found to be true both in terms of J_{IC} and J_{ss}. The toughening effect of rubber was consistent with increased plasticity observed on fracture surfaces.

2. The presence of rubber triggered *R*-curve behaviour in the unreinforced materials. The magnitude of toughening during the crack growth stage as a result of rubber addition was significantly larger than the magnitude of rubber toughening associated with the crack initiation stage. In the absence of rubber, no *R*-curve behaviour was found in the unreinforced blends. The rigid (non-elastomeric) polymer component as a minor phase addition did not trigger any *R*-curve behaviour.

3. In fact, addition of the second rigid phase always resulted in embrittlement. This is believed to be related to debonding at the rigid/rigid polymer interfaces. If the interface could be strengthened, toughening could be the result. The extent of this embrittlement was the same both in the presence and in the absence of rubber.

4. The role played by glass fibres was found to be critically related to the fibre/matrix interfacial strength. Toughening was generally observed, both in the presence and absence of rubber, when the interface was strong. Also, in the absence of rubber, addition of glass fibres always triggered *R*-curve behaviour, provided the interface was adequately strong. In the nylon 6,6 rich blend, however, the presence of rubber and fibres together resulted in the elimination of *R*-curve behaviour. This unusual result requires further study. In particular, there needs to be a better understanding of the conditions that induce *R*-curve behaviour in polymer alloys and composites.

5. Some direct evidence was presented of the ability of fibres to enhance plastic deformation in the matrix phase. The enhancement of plastic deformation was associated with the role of fibres in increasing the

deviatoric component of stress locally in the vicinity of fibre/matrix interfaces. In this respect, fibres were observed to behave much like rubber particles.

Acknowledgements

This project was supported by the National Science Foundation under grant MSS-9201625. The support from Monsanto Chemical Company, in terms of raw materials, processing facilities and microscopy, is acknowledged. The assistance provided by Mr Larry Gustafson for processing, and Dr Dave Alward, for the microscopy is also greatly appreciated.

References

1. B. MAJUMDAR, H. KESKULA and D. R. PAUL, *Polymer* **35** (1994) 5453.
2. B. MAJUMDAR, H. KESKULA and D. R. PAUL, *J. Polym. Sci. B Polym. Phys.* **32** (1994) 2127.
3. A. F. YEE and R. A. PEARSON, *J. Mater. Sci.* **21** (1986) 2462.
4. R. A. PEARSON and A. F. YEE, *ibid.* **21** (1993) 2474.
5. A. F. YEE, D. LI and X. LI, *ibid.* **28** (1993) 6392.
6. C. B. BUCKNALL, A. KARPODINIS and X. C. ZHANG, *ibid.* **29** (1994) 3377.
7. A. LAZZARI and C. B. BUCKNALL, *ibid* **28** (1993) 6799.
8. K. DIJKSTRA and G. H. TEN BOLSCHER, *ibid* **29** (1994) 4286.
9. K. DIJKSTRA, A. VAN DER WAL and R. J. GAYMANS, *ibid.* **29** (1994) 3489.
10. D. S. PARKER, H. J. SUE, J. HUANG and A. F. YEE, *Polymer* **31** (1990) 2267.
11. H. J. SUE and A. F. YEE, *J. Mater. Sci.* **24** (1989) 1447.
12. A. J. KINLOCH, S. J. SHAW, D. A. TOD and D. L. HUNSTON, *Polymer* **24** (1983) 1341.
13. P. BEAHAN, A. THOMAS and M. BEVIS, *J. Mater. Sci.* **11** (1976) 1207.
14. A. LAZZERI and C. B. BUCKNALL, *ibid.* **28** (1993) 6799.
15. N. C. LIU and W. E. BAKER, *Polym. Engng Sci.* **22** (1987) 3417.
16. S. V. NAIR, S. C. WONG and L. A. GOETTLER, *J. Mater. Sci.* **32** (1997) 5335.
17. "A Testing Protocol for Conducting J-Crack Growth Resistance Curve Tests in Plastics" (ASTM, West Conshohacken, PA, 1992).
18. V. C. LI, C. M. CHAN and C. K. Y. LEUNG, *Cem. Concr. Res.* **17** (1987) 441.
19. T. HASHIDA and V. C. LI, *J. Amer. Ceram. Soc.* **77** (1994) 1553.
20. T. HASHIDA and V. C. LI, *J. Amer. Ceram. Soc.* **77** (1994) 1553.
21. B. H. KIM and C. R. JOE, *Engng Fract. Mech.* **34** (1989) 221.
22. M. L. SHIAO, S. V. NAIR, P. D. GARRETT and R. E. POLLARD, *J. Mater. Sci.* **29** (1994) 739.
23. S. V. NAIR, M. L. SHIAO and P. D. GARRETT, *ibid.* **22** (1992) 1085.
24. M. L. SHIAO, S. V. NAIR, P. D. GARRETT and R. E. POLLARD, *Polymer* **35** (1994) 306.
25. S. V. NAIR, A. SUBRAMANIAM and L. A. GOETTLER, *J. Mater. Sci.*, 6335.
26. S. C. KUNZ, P. W. R. BEAUMONT and M. F. ASHBY, *ibid.* **15** (1980) 1109.
27. A. G. EVANS, Z. B. AHMAD, D. G. GILBERT and P. W. R. BEAUMONT, *Acta Metall.* **34** (1986) 1.
28. S. V. NAIR, A. SUBRAMANIAM and L. A. GOETTLER, *J. Mater. Sci.*, to be submitted.

Received 10 October 1996
and accepted 1 May 1997